

---

# Quantum Monte Carlo Calculations for Ground and Excited States

---

R. J. NEEDS, P. R. C. KENT,\* A. R. PORTER, M. D. TOWLER,  
G. RAJAGOPAL

*TCM Group, Cavendish Laboratory, Madingley Road, Cambridge CB3 0HE, United Kingdom*

*Received 4 October 2000; revised 2 May 2001; accepted 3 May 2001*

---

**ABSTRACT:** A brief overview of the diffusion quantum Monte Carlo method is given. We illustrate the application to ground-state calculations by a study of the relative stability of carbon clusters near the crossover to fullerene stability, thereby determining the smallest stable fullerene. The application to excited states is illustrated via a study of excitonic states in small hydrogenated silicon clusters. © 2002 John Wiley & Sons, Inc. *Int J Quantum Chem* 86: 218–225, 2002

**Key words:** diffusion quantum Monte Carlo; fullerenes; hydrogenated silicon clusters; ground states; excited states

---

## Introduction

A sophisticated description of electron correlation is required to describe the structures, energetics, and properties of molecules and solids. The fixed-node diffusion quantum Monte Carlo (DMC) method [1–3] is a stochastic technique for solving the many-body Schrödinger equation with an accurate treatment of electron correlation. Highly accurate DMC calculations of ground-state energies have already been demonstrated [1–5] and in principle such accuracy can also be attained for excited states. The great promise of these methods lies in the fact that electron–electron correlations are included

explicitly, essentially without approximation, and that the computational cost increases as the third power of the number of electrons, which is very favorable when compared with other correlated wave function techniques.

In this study we give a brief overview of the DMC method and describe its application to two problems. The first application is to a ground-state problem; the relative stability of carbon clusters near the crossover to where fullerene molecules have become stable [6]. The second is an application to the excitonic states of small hydrogenated silicon clusters [7].

---

## The DMC Method

The DMC method is a stochastic projector method for evolving the imaginary-time Schrö-

*Correspondence to:* R. Needs; e-mail: rn11@phy.cam.ac.uk.

\*Present address: National Renewable Energy Laboratory, Golden, Colorado 80401, USA.

Contract grant sponsor: EPSRC (UK).

dinger equation,

$$-\frac{\partial \Psi(\mathbf{R}, t)}{\partial t} = (\hat{H} - E_S)\Psi(\mathbf{R}, t), \quad (1)$$

where  $t$  is a real variable measuring the progress in imaginary time, and  $E_S$  is an energy offset. This equation has the property that an initial starting state decays toward the ground-state wave function (provided they have a nonzero overlap). The time evolution of Eq. (1) may be followed using a stochastic technique. The wave function  $\Psi(\mathbf{R}, t)$  is represented by an ensemble of  $3N$ -dimensional electron configurations,  $\{\mathbf{R}_i\}$ , whose time evolution is governed by Eq. (1). The Green function of Eq. (1) shows that the rules of the evolution are random diffusive jumps of the configurations arising from the kinetic term and removal/addition of configurations arising from the potential energy term.

Unfortunately, this simple algorithm suffers from two serious problems. The first is that we have implicitly assumed that  $\Psi$  is a probability distribution, even though its fermionic nature means that it must have positive and negative parts. The second problem is less fundamental but in practice very severe. The required rate of removing/adding configurations diverges when the potential energy diverges, which occurs whenever two electrons or an electron and a nucleus are coincident, leading to poor statistical behavior.

To deal with the first problem we use the *fixed-node approximation* [8]. The nodal surface of a wave function is the surface on which it is zero and across which it changes sign. If we force the time evolution of Eq. (1) to maintain a nodal surface consistent with the fermionic antisymmetry, we can simulate the equation separately in each nodal pocket. The fixed nodal surface can be imposed by considering the evolution of the *mixed distribution*  $f = \Phi_T \Psi$ , where  $\Phi_T$  is known as the trial or guiding wave function. The nodal surface of  $\Psi$  is constrained to be the same as that of  $\Phi_T$  and therefore  $f$  can be interpreted as a probability distribution and the evolution generates the distribution  $f = \Phi_T \Psi$ , where  $\Psi$  is the best (lowest energy) wave function with the same nodes as  $\Phi_T$ . The second problem is also dealt with by the introduction of the  $f$  distribution, which introduces *importance sampling* and greatly reduces the statistical noise. Normally we demand that  $\Phi_T$  has the correct cusplike behavior when two electrons or an electron and a nucleus are coincident [9], which removes the divergence in the removal/addition process.

The fixed-node approximation implies that we solve independently in different nodal pockets, and at first sight it appears that we have to solve the Schrödinger equation in every nodal pocket, which would be an impossible task in large systems. However, the *tiling theorem* for fermion ground states [10, 11] asserts that all nodal pockets are in fact equivalent and therefore one only need solve the Schrödinger equation in one of them. This theorem is intimately connected with the existence of a variational principle for the DMC ground-state energy [11]. There are no generally applicable tiling or variational theorems for excited states, and there may not even be tiling or variational theorems for the lowest energy state of each symmetry [11]. It is straightforward to show that if the trial wave function has the exact nodal surface of an excited state, then the DMC algorithm gives the exact energy of that state. The DMC method gives the lowest energy consistent with the nodal surface of the trial wave function, and therefore by using a trial wave function with a nodal surface close to that of an excited state we can obtain an accurate estimate of the energy of the excited state. Excited-state DMC calculations of this type have been performed for both small molecules [7, 12] and extended systems [13, 14]. The absence of a tiling theorem for an excited state means that in principle the energy could depend on the nodal pockets within which the Schrödinger equation is solved. However, experience shows that provided the trial wave function is sufficiently accurate the loss of the tiling theorem normally has an insignificant effect.

A DMC simulation proceeds as follows. First we pick an ensemble of a few hundred configurations chosen from the distribution  $|\Phi_T|^2$  using the standard Metropolis algorithm. This ensemble is evolved in imaginary time according to the rules of the importance sampled imaginary time Schrödinger equation, which involves biased diffusion and addition/subtraction steps. The bias in the diffusion is caused by the importance sampling, which directs the sampling toward parts of configuration space where  $\Phi_T$  is large. After a period of equilibration the configurations start to trace out the probability distribution  $f(\mathbf{R}) / \int f(\mathbf{R}) d\mathbf{R}$ . We can then start to accumulate averages, in particular the DMC energy,  $E_D$ , which is given by

$$E_D = \frac{\int f(\mathbf{R}) E_L(\mathbf{R}) d\mathbf{R}}{\int f(\mathbf{R}) d\mathbf{R}} \approx \sum_i E_L(\mathbf{R}_i), \quad (2)$$

$E_L = \Phi_T(\mathbf{R})^{-1} \hat{H} \Phi_T(\mathbf{R})$  is known as the local energy and the configurations are distributed according to

$f(\mathbf{R})/\int f(\mathbf{R})d\mathbf{R}$ . This energy expression would be exact if the nodal surface of  $\Phi_T$  was exact, and the fixed-node error is second order in the error in the nodal surface of  $\Phi_T$  (when a variational theorem exists). The accuracy of the fixed-node approximation can be tested on small systems and normally leads to very satisfactory results [2].

The trial wave function limits the final accuracy that can be obtained because of the fixed-node approximation, and it also controls the statistical efficiency of the algorithm. The DMC algorithm satisfies a zero-variance principle, i.e., the variance of the energy goes to zero as the trial wave function goes to an exact eigenstate. It is essential to have a reasonably accurate trial wave function, and we use trial wave functions of the Slater–Jastrow form:

$$\Psi = \left( \sum_i c_i \mathcal{D}_i^\uparrow \mathcal{D}_i^\downarrow \right) \exp(\mathcal{J}), \quad (3)$$

where  $\exp(\mathcal{J})$  is the Jastrow factor and  $\mathcal{D}_i^\uparrow$  and  $\mathcal{D}_i^\downarrow$  are Slater determinants of one-particle up-/down-spin orbitals. We use Jastrow factors, which correlate the motion of pairs of electrons, although higher body correlations can also be included. The Jastrow factor normally includes a number of parameters whose values may be varied to optimize the wave function [15, 16]. The Slater determinants of one-particle orbitals are usually obtained from Hartree–Fock (HF) or density functional theory (DFT) calculations or from multideterminant quantum chemical calculations.

Although the computational cost of a DMC calculation increases as only the third power of the number of electrons, it increases much more rapidly with the nuclear charge,  $Z$ , of the atoms. Estimates range from a  $Z^{5.5}$  scaling [17] to  $Z^{6.5}$  [18], which rules out applications to heavy atoms. It is therefore normal to use pseudopotentials in DMC calculations, which act to reduce the effective value of  $Z$ . Norm-conserving nonlocal DFT pseudopotentials often give very satisfactory results, although HF pseudopotentials are a little better. Unfortunately the fixed-node approximation conflicts with the use of nonlocal pseudopotentials and so an approximation known as the locality or localization approximation [19] is made, which normally works very well.

The quality of the Slater part of the Slater–Jastrow wave function is crucial because it usually accounts for in excess of 90% of the electronic energy. For closed-shell ground states, a single pair of up-/down-spin determinants is normally sufficient, but for excited states a multideterminant trial wave

function may be necessary. DMC is a real-space technique and the repeated evaluation of the trial wave function (and its gradient and Laplacian) at many different points in configuration space is the most costly part of the calculation. One would like to be able to evaluate the orbitals and their derivatives at arbitrary points in real space as rapidly as possible, and therefore the representation of the single-particle orbitals is important for computational efficiency. One possibility is to store them on grids and interpolate, but for large systems this requires too much storage. A good compromise is to use a localized basis set to represent the single-particle orbitals and the most common choice is a set of Cartesian Gaussian functions. The great advantage of this representation is that one can interface the DMC code directly to Gaussian orbital quantum chemistry software packages such as CRYSTAL [20] or GAUSSIAN [21]. All of the DMC calculations reported here used the CASINO [22] quantum Monte Carlo code.

This completes our brief introduction to the DMC method. We have left out many technical details of the calculations, and for more information on these aspects the reader is directed to Refs. [2, 3].

---

## Application to Ground States: Carbon Clusters

The discovery and synthesis of the  $C_{60}$  fullerene [23] has aroused a great deal of interest. Fullerene clusters can now be synthesized in macroscopic quantities that may lead to the development of new and useful materials. The main technique for producing small carbon clusters is laser vaporization of graphite followed by an annealing process, which produces a broad spectrum of cluster sizes. Other synthesis routes are also possible, and, for instance, the smallest possible fullerene ( $C_{20}$ ) was recently synthesized from hydrogenated  $C_{20}H_{20}$  cluster by exposure to bromine [24].

Mass spectra of  $C_n$  clusters produced by laser vaporization of graphite show many clusters with  $10 \leq n \leq 18$ , consisting mostly of monocyclic rings, and  $32 \leq n \leq 60$ , consisting mostly of fullerene molecules [25, 26]. All of these clusters are metastable in the sense that they have higher energies per atom than graphite, but they are believed to be the lowest energy isomers for these values of  $n$ . It is now widely believed that the fullerenes formed by this procedure develop via a “fullerene road”

mechanism [27, 28] in which small fullerenes grow by the addition of carbon atoms.

We have attempted to establish the energetic ordering of the even-numbered clusters near the crossover to fullerene stability, thereby allowing us to answer the question: Which is the smallest stable fullerene? This could shed light on the start of the fullerene road and indicate limitations on which isomers can be produced by laser vaporization. We have studied carbon clusters containing 24, 26, 28, and 32 atoms for which three classes of isomer are energetically competitive: fullerenes, planar or near-planar sheets and bowls, and monocyclic rings. The number of candidate low-energy structures is large, and therefore a hierarchy of methods of increasing accuracy and computational cost is used to identify them. The initial selection, based on simple bond counting and geometric rules, is refined using quantum mechanical tight-binding [29] and density functional theory (DFT) calculations [30–33]. The final energetic ordering is established using the DMC method. A number of earlier studies have demonstrated the need for highly accurate calculations for obtaining the correct energetic ordering of the clusters. For example, the DMC study of  $C_{20}$  by Grossman et al. [34] showed that the fullerene is not the most energetically stable isomer, contradicting the predictions of earlier less accurate DFT calculations.

As well as DMC calculations we have also performed DFT calculations using the local density approximation (LDA), two gradient-corrected functionals (PBE [35] and BLYP [36]), and a hybrid functional (B3LYP) [37]. The DFT calculations

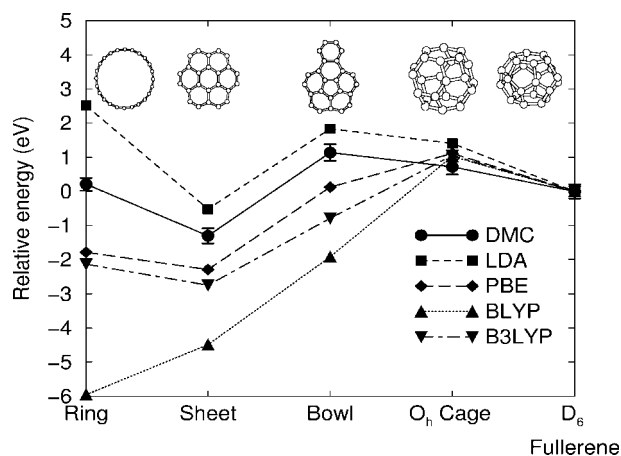


**FIGURE 1.** Structures and energies of the  $C_{24}$  isomers given relative to the  $D_6$  fullerene.

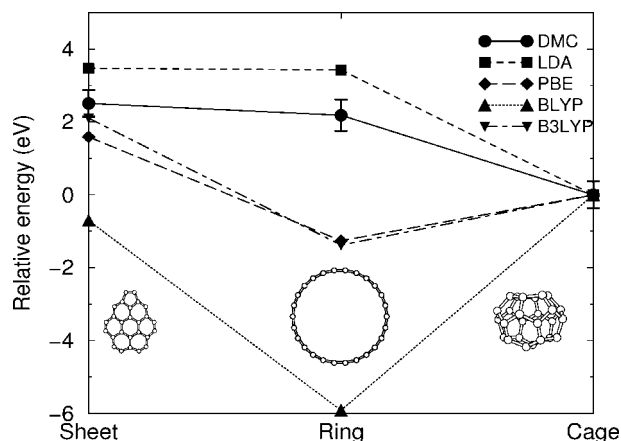


**FIGURE 2.** Structures and energies of the  $C_{26}$  isomers, given relative to the cage structure.

were performed using the CRYSTAL95 [20] and GAUSSIAN [21] codes. Relaxed geometries were obtained from DFT calculations using the B3LYP hybrid density functional and a large Gaussian basis set. Tests show that although the relaxed geometries are rather insensitive to the choice of density functional, this is not the case for the energetic ordering of the clusters (see Figs. 1–3). For the trial wave functions we used a single pair of up-/down-spin determinants, except for the  $C_{26}$  ring where we used a 43-determinant trial wave function obtained from a configuration interaction calculation with single and double excitations. Recently, Torelli and Mitas have demonstrated the importance of using multideterminant wave functions to describe the aromatic nature of  $n = 4N + 2$  carbon rings [38]

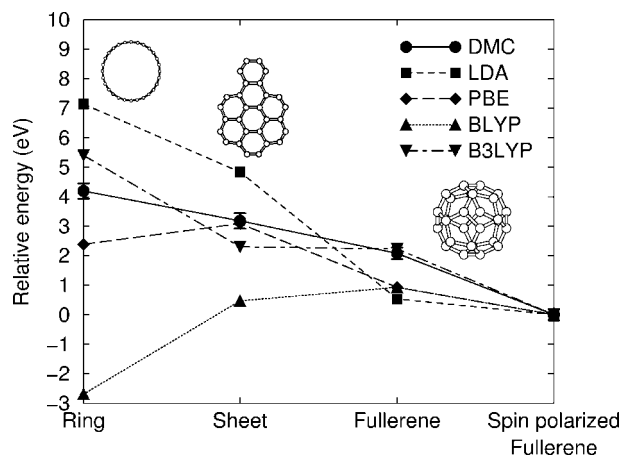


**FIGURE 3.** Structures and energies of the  $C_{28}$  isomers, given relative to the spin-polarized fullerene.

with  $N = 1 - 4$ , but the effect decreases for larger  $N$  and we did not find it very important for  $C_{26}$ .

The results shown in Figures 1–3 show that the treatment of correlation has a significant effect on the relative energies. All of the density functionals give different orderings of the energies, and none gives the same ordering as DMC. For  $C_{24}$  our DMC calculations predict the graphitic sheet to be lowest in energy, being 1.3(2) eV more stable than the  $D_6$  fullerene and ring structures. The low energy of the  $C_{24}$  graphitic sheet is expected because the structure is compact and accommodates a large number of hexagonal rings without significant strain. As smaller graphitic sheets are high in energy [33], the  $C_{24}$  sheet is expected to be the smallest stable graphitic fragment. For  $C_{26}$  the ring and sheetlike isomers are close in energy, but the fullerene is 2.2(4) eV lower in energy and is therefore predicted to be the most stable  $C_{26}$  isomer and the smallest stable fullerene. The  $C_{28}$   $T_d$  symmetry fullerene was found to be spin-polarized, in agreement with earlier DFT and HF calculations. The spin-polarized  $C_{28}$  fullerene is 4.2(3) eV lower in energy than the ring and 3.2(3) eV lower than the sheet. This indicates that isolated  $C_{28}$  fullerenes might be produced, possibly facilitating the production of  $C_{28}$  fullerene solids [39, 40]. Our DMC calculations for the  $C_{32}$  monocyclic ring and fullerene show that the fullerene is 8.4(4) eV per molecule lower in energy, which is consistent with the observation of a large abundance of  $C_{32}$  fullerenes in a recent cluster experiment [25].

In summary, this study has further demonstrated the need for an accurate description of electron correlation for the carbon cluster problem. We find the lowest energy isomer of  $C_{24}$  to be a graphitic sheet, which is expected to be the smallest stable graphitic fragment. Our DMC results, combined with those of Grossman et al. [34], predict a small window of stability for sheet/bowl structures around 20–24 atoms. We predict that the smallest energetically stable fullerenes are the  $C_{2v}$  symmetry  $C_{26}$  cluster and the reactive, spin-polarized  $C_{28}$  cluster.

---

### Application to Excited States: Hydrogenated Silicon Clusters

Hydrogenated silicon clusters may be used to model the absorption and emission of light in quantum dots [41] and porous silicon [42]. The optical properties of these clusters are greatly influenced by the strong electron–hole interactions arising from

quantum confinement, and the accurate prediction of their excitonic gap energies is a very challenging theoretical problem. These systems have become important for benchmarking excitation energy calculations and studies using many methods have been reported, including empirical tight-binding techniques, first-principles local density functional methods, and many-body perturbation theory techniques. We have calculated the excitonic states of  $SiH_4$ ,  $Si_2H_6$ ,  $Si_5H_{12}$ , and  $Si_{10}H_{16}$  clusters using the DMC technique.

We noted earlier that the quality of the trial wave function is crucial for the success of a DMC calculation. For the ground states of the carbon clusters discussed in the previous section, only a single pair of up- and down-spin determinants was required, but to describe some of the excited states of these small hydrogenated silicon clusters it is essential to use a multideterminant description. There are a number of quantum chemical methods that could be used to obtain such a wave function, but we have chosen to investigate the singles-only configuration interaction (CIS) method [43]. CIS wave functions consist of a linear combination of determinants involving only single excitations from the ground state. These wave functions can therefore be resummed into a number of determinants equal to the number of electrons in the system, which makes the DMC calculations much more efficient. Such wave functions can give a reasonable zeroth-order description of the strong electron–hole interactions that occur in hydrogenated silicon clusters.

For all of the CIS calculations in this study we used the GAUSSIAN [21] package. Results for the absorption spectra of the clusters calculated within CIS are shown in Figure 4. The lowest absorption energy decreases with increasing cluster size because of the reduction in quantum confinement. Note also that the absorption for the  $Si_{10}H_{16}$  cluster is very weak in the low energy region.

In Figure 5 we plot the DMC and CIS energies of the lowest triplet and the lowest bright (dipole-allowed) singlet transitions against cluster size, together with the available experimental data. The CIS singlet excitation energies are too high because the correlation energy, which is poorly described in CIS, is larger in the excited states than in the ground state. CIS also overestimates the singlet-triplet splitting because, for the triplet, electron–hole correlation is dominated by the exchange interaction, which is well described by CIS, while for the singlet the electron–hole correlation is more important. The DMC singlet energies are lower than the CIS values,

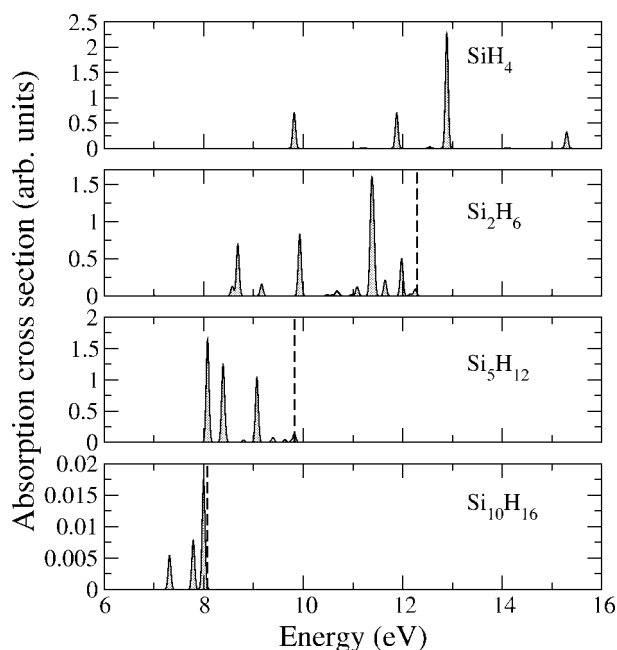


**FIGURE 4.** Absorption spectra of  $\text{Si}_n\text{H}_m$  clusters calculated within CIS and artificially broadened by 0.04 eV. The vertical dashed lines indicate the highest energy to which the spectra were calculated.

although still a little larger than the experimental ones. The comparison with experiment is unfortunately not straightforward because of the breadth of the measured absorption peaks and the likely

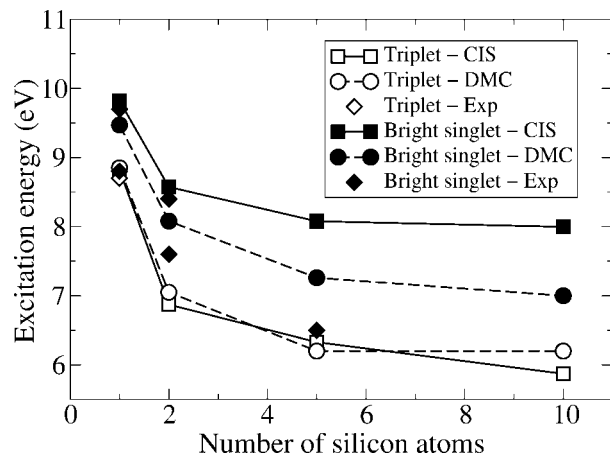


**FIGURE 5.** Energies of the lowest triplet and bright (dipole-allowed) singlet transitions from CIS and DMC calculations together with the available experimental data, versus cluster size. The experimental data for the singlet states of  $\text{SiH}_4$  and  $\text{Si}_2\text{H}_6$  is from Itoh et al. [44], while for  $\text{Si}_5\text{H}_{12}$  it is from Fehér [45], while the data for the triplet state of  $\text{SiH}_4$  is from Curtis and Walker [46].

role of vibrational and Jahn–Teller effects. All of the excited states shown in Figure 5 are orbitally degenerate and therefore subject to Jahn–Teller distortions, which are not included in our calculations and would tend to reduce the calculated lowest excitation energies. One cannot rule out other possibilities such as effects due to the vibrational energy levels, or some residual bias due to the use of CIS trial wave functions in the DMC calculations. Our DMC values for the excitation energies are a little higher than those of Rohlfiing and Louie [47], who solved the Bethe–Salpeter equation (BSE) using the results of GW self-energy calculations. Recently, however, these authors have found that the neglect of the off-diagonal matrix elements of the self-energy in their work led to some inaccuracies, and that inclusion of these terms increased the lowest singlet and triplet excitation energies of  $\text{SiH}_4$  by 0.4 and 0.8 eV [48], respectively, which brings their results into much better agreement with ours. Grossman et al. [48] also calculated excitation energies of  $\text{SiH}_4$  using the DMC method, obtaining results in good agreement with ours.

In summary, we have shown that the DMC method, combined with suitable methods for generating trial wave functions, is a viable and accurate method for calculating the excited states of hydrogenated silicon clusters. The need for sophisticated trial wave functions has been emphasized and we have shown that the quantum chemical CIS technique can provide suitable zeroth-order approximations in these systems. CIS wave functions have properties that make them highly suitable for use in DMC calculations, and they are sufficiently computationally tractable to allow the construction of accurate trial wave functions for quite large systems. The techniques described here will therefore allow application of the DMC method to excited states of a broad range of systems with strong electron–hole interactions.

## Conclusions

In conclusion, we have given a brief overview of the diffusion quantum Monte Carlo method and described how it provides a unified framework for studying ground and excited states. We have described the application of the DMC method to two problems in cluster science: the ground-state energies of carbon clusters and excited-state energies of hydrogenated silicon clusters. The DMC method is reliant on the availability of a reasonably accu-

rate trial wave function, and for many purposes the Slater–Jastrow form is sufficient. For closed-shell ground states a single determinant of Hartree–Fock or local density approximation (LDA) orbitals is often sufficient, although for excited states multideterminant wave functions are sometimes necessary. We have found that a multideterminant CIS wave function gives a good trial wave function for excited states of hydrogenated silicon clusters.

### ACKNOWLEDGMENTS

Financial support was provided by EPSRC (UK). Computational resources on a COMPAQ multiprocessor machine (Columbus cluster), provided by UK Computational Chemistry Facility at the Rutherford Appleton Laboratory (admin.: Department of Chemistry, King’s College London, Strand, London WC2R 2LS) are acknowledged. Most of the DMC calculations were performed on the CRAY-T3E administered by CSAR at the University of Manchester and the Hitachi SR2201 located at the University of Cambridge High Performance Computing Facility.

### References

- Ceperley, D. M.; Alder, B. J. *Phys Rev Lett* 1980, 45, 566.
- Hammond, B. L.; Lester, W. A.; Reynolds, P. J. *Monte Carlo Methods in Ab Initio Quantum Chemistry*; World Scientific: Singapore, 1994.
- Foulkes, W. M. C.; Mitas, L.; Needs, R. J.; Rajagopal, G. *Rev Mod Phys* 2001, 73, 33.
- Filippi, C.; Umrigar, C. J. *J Chem Phys* 1996, 105, 213.
- Kent, P. R. C.; Hood, R. Q.; Williamson, A. J.; Needs, R. J.; Foulkes, W. M. C.; Rajagopal, G. *Phys Rev B* 1999, 59, 1017.
- Kent, P. R. C.; Towler, M. D.; Needs, R. J.; Rajagopal, G. *Phys Rev B* 2000, 62, 15394.
- Porter, A. R.; Towler, M. D.; Needs, R. J. *Phys Rev B* 2001, 64, 035320.
- Anderson, J. B. *J Chem Phys* 1975, 63, 1499.
- Kato, T. *Comm Pure Appl Math* 1957, 10, 151.
- Ceperley, D. *J Stat Phys* 1991, 63, 1237.
- Foulkes, W. M. C.; Hood, R. Q.; Needs, R. J. *Phys Rev B* 1999, 60, 4558.
- Grimes, R. M.; Hammond, B. L.; Reynolds, P. J.; Lester, W. A. *J Chem Phys* 1986, 85, 4749.
- Williamson, A. J.; Hood, R. Q.; Needs, R. J.; Rajagopal, G. *Phys Rev B* 1998, 57, 12140.
- Towler, M. D.; Hood, R. Q.; Needs, R. J. *Phys Rev B* 2000, 62, 2330.
- Umrigar, C. J.; Wilson, K. G.; Wilkins, J. W. *Phys Rev Lett* 1988, 60, 1719.
- Kent, P. R. C.; Needs, R. J.; Rajagopal, G. *Phys Rev B* 1999, 59, 12344.
- Ceperley, D. M. *J Stat Phys* 1986, 43, 815.
- Hammond, B. L.; Reynolds, P. J.; Lester, W. A. *J Chem Phys* 1987, 87, 1130.
- Hurley, M. M.; Christiansen, P. A. *J Chem Phys* 1987, 86, 1069; Hammond, B. L.; Reynolds, P. J.; Lester, W. A. *J Chem Phys* 1987, 87, 1130; Mitas, L.; Shirley, E. L.; Ceperley, D. M. *J Chem Phys* 1991, 95, 3467.
- Saunders, V. R.; Dovesi, R.; Roetti, C.; Causá, M.; Harrison, N. M.; Orlando, R.; Zicovich-Wilson, C. M. *CRYSTAL98 User’s Manual*; University of Torino: Torino, 1998.
- Frisch, M. J.; Trucks, G. W.; Schlegel, H. B.; Scuseria, G. E.; Robb, M. A.; Cheeseman, J. R.; Zakrzewski, V. G.; Montgomery, J. A.; Stratmann, R. E.; Burant, J. C.; Dapprich, S.; Millam, J. M.; Daniels, A. D.; Kudin, K. N.; Strain, M. C.; Farkas, O.; Tomasi, J.; Barone, V.; Cossi, M.; Cammi, R.; Mennucci, B.; Pomelli, C.; Adamo, C.; Clifford, S.; Ochterski, J.; Petersson, G. A.; Ayala, P. Y.; Cui, Q.; Morokuma, K.; Malick, D. K.; Rabuck, A. D.; Raghavachari, K.; Foresman, J. B.; Cioslowski, J.; Ortiz, J. V.; Stefanov, B. B.; Liu, G.; Liashenko, A.; Piskorz, P.; Komaromi, I.; Gomperts, R.; Martin, R. L.; Fox, D. J.; Keith, T.; Al-Laham, M. A.; Peng, C. Y.; Nanayakkara, A.; Gonzalez, C.; Challacombe, M.; Gill, P. W. M.; Johnson, B. G.; Chen, W.; Wong, M. W.; Andres, J. L.; Head-Gordon, M.; Replogle, E. S.; Pople, J. A. *Gaussian 98, Revision A.9*; Gaussian, Inc.: Pittsburgh, PA, 1998.
- Needs, R. J.; Rajagopal, G.; Towler, M. D.; Kent, P. R. C.; Williamson, A. J. *CASINO version 1.0 User’s Manual*; University of Cambridge: Cambridge, 2000.
- Kroto, H. W.; Heath, J. R.; O’Brien, S. C.; Curl, R. F.; Smalley, R. E. *Nature (London)* 1985, 318, 162.
- Prinzbach, H.; Weller, A.; Landenberger, P.; Wahl, F.; Wörth, J.; Scott, L. T.; Gelmont, M.; Olevano, D.; Issendorff, B. *Nature (London)* 2000, 407, 60.
- Kietzmann, H.; Richow, R.; Ganteför, G.; Eberhardt, W.; Vietze, K.; Seifert, G.; Fowler, P. W. *Phys Rev Lett* 1998, 81, 5378.
- Handschuh, H.; Ganteför, G.; Kessler, B.; Bechthold, P. S.; Eberhardt, W. *Phys Rev Lett* 1995, 74, 1095.
- Heath, J. R. *ACS Symp Ser* 1992, 481.
- Fowler, P. W.; Manolopoulos, D. E. *An Atlas of Fullerenes*; Clarendon Press: Oxford, 1995.
- Cioslowski, J. *Electronic Structure Calculations on Fullerenes and Their Derivatives*; Oxford University Press: 1995.
- Martin, J. M. L. *Mol Phys* 1995, 86, 1437.
- Martin, J. M. L. *Chem Phys Lett* 1996, 255, 1.
- Scuseria, G. E. *Science* 1996, 271, 942.
- Jones, R. O. *J Chem Phys* 1999, 110, 5189.
- Grossman, J. C.; Mitas, L.; Raghavachari, K. *Phys Rev Lett* 1995, 75, 3870; Erratum: *Phys Rev Lett* 1995, 76, 1006.
- Perdew, J. P.; Burke, K.; Ernzerhof, M. *Phys Rev Lett* 1996, 77, 3865.
- Becke, A. D. *Phys Rev A* 1988, 38, 3098; Lee, C.; Yang, W.; Parr, R. G. *Phys Rev B* 1988, 37, 785.
- Becke, A. D. *J Chem Phys* 1993, 98, 5648.
- Torelli, T.; Mitas, L. *Phys Rev Lett* 2000, 85, 1702.

39. Guo, T.; Diener, M. D.; Chai, Y.; Alford, M. J.; Haufler, R. E.; McClure, S. M.; Ohno, T.; Weaver, J. H.; Scuseria, G. E.; Smalley, R. E. *Science* 1992, 257, 1661.
40. Kim, J.; Galli, G.; Wilkins, J. W.; Canning, A. *J Chem Phys* 1998, 108, 2631.
41. Wolkin, M. V.; Jorne, J.; Fauchet, P. M.; Allen, G.; Delerue, C. *Phys Rev Lett* 1999, 82, 197.
42. Canham, L. T. *Appl Phys Lett* 1990, 57, 1046.
43. Foresman, J. B.; Head-Gordon, M.; Pople, J. A.; Frisch, M. J. *J Phys Chem* 1992, 96, 135.
44. Itoh, U.; Toyoshima, Y.; Onuki, H. *J Chem Phys* 1986, 85, 4867.
45. Fehér, F. *Molekülspektroskopische Untersuchungen auf dem Gebiet der Silane und der Heterocyclischen Sulfane*, Forschungsbericht des Landes Nordrhein-Westfalen; West-Deutscher: Köln, 1977.
46. Curtis, M. G.; Walker, I. C. *J Chem Soc Faraday Trans* 1989, 85, 659.
47. Rohlfing, M.; Louie, S. G. *Phys Rev Lett* 1998, 80, 3320.
48. Grossman, J.; Rohlfing, M.; Mitas, L.; Louie, S. G.; Cohen, M. L. *Phys Rev Lett* 2001, 86, 472.